



Combining high-throughput experimentation, advanced data modeling and fundamental knowledge to develop catalysts for the epoxidation of large olefins and fatty esters

Pedro Serna, Laurent A. Baumes, Manuel Moliner, Avelino Corma*

Instituto de Tecnología Química, UPV-CSIC, Universidad Politécnica de Valencia, Avda. de los Naranjos s/n, 46022 Valencia, Spain

ARTICLE INFO

Article history:

Received 1 April 2008

Revised 22 May 2008

Accepted 23 May 2008

Available online 7 July 2008

Keywords:

Epoxidation

Ti-MCM-41

Ti-ITQ-2

Silylating agents

High-throughput

Molecular modeling

Test reaction

ABSTRACT

By combining catalyst characterization, molecular descriptors, and high-throughput techniques, two structured titanosilicates, Ti-MCM-41 and Ti-ITQ-2, were successfully optimized for the epoxidation of large olefins and methyl oleate. This new methodology for material science and catalysis can help to identify and partially quantify the roles of the variables involved in catalyst synthesis based on a small number of experiments. Associations among the chemical properties of the silicate used as support (ITQ-2, MCM-41), the dispersion and number of Ti sites grafted onto the surface, the presence of surface modifiers (silylating agents), the nature of the selected alkenes, and the catalytic activity and selectivity are established. We show that the use of surface modifiers increases the activity and selectivity of the catalysts, but that the effectiveness of each silylating agent depends on the surface characteristics of the support. Correlation of the results from the epoxidation of a test molecule, 4-decene with those for the industrially relevant methyl oleate show that the reactivity of the substrate also is significantly influenced by the surface properties of the support. We find that Ti-ITQ-2 modified with SiMe₂Bu (dimethylbutylsilane), instead of the more commonly used Ti-MCM-41–SiMe₃ system (with trimethylsilane as a silylating agent), represents the best option for carrying out the epoxidation of this fatty ester, leading to a highly active and selective catalyst.

© 2008 Elsevier Inc. All rights reserved.

1. Introduction

The use of biomass as raw material for chemicals, fine chemicals, petrochemicals, and fuel applications has become a relevant scientific and technical issue in recent years [1]. Recent work has focused on the transformation of natural fats and oils into alkanes by hydrotreatment [2] and in the preparation of methyl esters of the fatty acids by transesterification with methanol [3]. Besides its wide range of direct applications in fuels, food, pharmaceuticals, and cosmetics, methyl oleate can be selectively oxidized to the corresponding epoxide, providing a very versatile product with applications for plasticizers, lubricants, and polymer stabilizers, among others. The current industrial scale process for obtaining these epoxides is based on the Prileschajew reaction [4], which involves undesirable mineral acids for catalyzing the oxidation of the double bond. Therefore, the development of new efficient and environmentally friendly heterogeneous catalysts as an alternative to the current technology [5] is of significant interest.

The discovery of titanosilicates as heterogeneous catalysts for epoxidation reactions [6] has encouraged the synthesis of new ti-

tanosilicate structures for epoxidizing different substrates [7]. For instance, in the case of long-chain olefins, such as methyl oleate, the accessibility of the reactant to the active sites requires application of titanosilicates with mesopores and/or, in general, the use of materials with large external surface areas. From the standpoint of the active sites, most emphasis has been placed on preparing titanosilicates in which the Ti is highly dispersed and preferably in a tetrahedral coordination [8]. Achieving adequate pore size and Ti coordination is a necessary, but not sufficient, prerequisite for obtaining a highly active, selective, and stable catalyst. Other catalyst characteristics (i.e., polarity and adsorption properties) must be considered as well. More specifically, it is known that Ti sites become deactivated in the presence of water if their SiO₂ environment is insufficiently hydrophobic. For instance, the catalytic behavior of Ti-MCM-41 with organic peroxides as oxidants can be greatly improved by increasing the hydrophobicity of the Ti through a silylation process [9]. But selecting the optimum silylation procedure is not an easy task, because the final catalytic performance will depend on the coupling between the nature of silylating agent, the nature of the titanosilicate surface, and the nature of the reactant. Taking these factors into account, it becomes apparent that the optimization of an epoxidation titanosilicate catalyst will involve a large number of preparations. Contributing to

* Corresponding author. Fax: +1 34 (96) 3877809.

E-mail address: acorma@itq.upv.es (A. Corma).

this difficulty is the lack of models to help predicting the most adequate catalyst formulation for a particular epoxidation reaction. Various approaches to applying high-throughput technologies to study epoxidation reactions have been reported in the literature [10].

We became interested in developing a specific strategy to further ease the experimental effort by combining high-throughput synthesis [11] and high-throughput catalytic testing [12] with fundamental characterization, molecular modeling [13], and quantitative structure activity and property analysis (QSAR and QSPR) [14]. However, investigations involving certain types of molecules can be experimentally annoying when routine laboratory tasks (e.g., weighting reagents, cleaning contaminated material, analyzing the composition of a reaction mixture) become tedious. Consider, for instance, methyl oleate, whose oily nature (high viscosity, high boiling point) complicates these tasks, increasing the cost of the research.

Under this scenario, we decided to start the research with an alternative olefin, 4-decene, which we used as a test molecule. From our approach, we expect to be able not only to optimize the catalyst, but also to gain a physicochemical understanding of the problem that, hopefully, can be transferred from the model reactant to feeds and reactants of industrial interest. More specifically, we explore how it is possible, by means of the methodology outlined above, to optimize an epoxidation catalyst for fatty esters in which the following catalyst variables are considered: (a) the nature of the support (structures mesoporous MCM-41 and delaminated zeolite ITQ-2), (b) the nature of the silylating agent (four molecules), (c) various loadings of silylating agent (six levels), and (d) the nature of the reactant (4-decene and methyl oleate). We find that delaminated zeolites, such as Ti-ITQ-2, provide better results than Ti-MCM-41 for reacting fatty substrates, such as methyl oleate, provided that the proper silylating agent at the optimum level is used to modify the surface properties of the silicate.

2. Experimental

2.1. Synthesis of supports: MCM-41, ITQ-2

MCM-41 and ITQ-2 were synthesized as described previously [15]. In preparing the MCM-41 support (see Fig. S1a in Supplementary material), amorphous silica (Aerosil 200, Degussa), a 25 wt% aqueous solution of tetramethylammonium hydroxide (Aldrich, 25 wt%), and an aqueous solution of hexadecyl-trimethylammonium bromide (CTMABr, Aldrich, purum) were used to prepare the starting synthesis gel. First, an appropriate amount of water was mixed with CTMABr and TMAOH, and the mixture was stirred until it was homogenized. Then Aerosil was added to form a new homogeneous gel after the compounds were mixed. The following molar composition was used to synthesize MCM-41: SiO_2 : 0.15 CTMA: 0.26 TMA: 0.26 OH: 24 H_2O . The crystallization was carried out in a Teflon autoclave at 135 °C for 24 h. After crystallization, the sample was washed and then dried at 60 °C for 12 h. Finally, the solid was calcined for 3 h at 540 °C in N_2 and then for 6 h in air.

The ITQ-2 (see Fig. S1b in Supplementary material) was prepared as follows. First, 10 g of the lamellar precursor ITQ-1 was dispersed in 40 g of H_2O milli-Q; then 200 g of a hexadecyl-trimethylammonium hydroxide solution (25 wt%, 50% exchanged Br/OH), and 60 g of a tetrapropylammonium hydroxide solution (40 wt%, 30% exchanged Br/OH) were added. The resulting mixture (pH \geq 12.5) was heated to 80 °C and stirred vigorously for 16 h, to facilitate swelling of the precursor material layers. At this point, the suspension was sonicated in an ultrasound bath (50 W, 50 Hz) for 1 h to disperse the individual sheets. Then the pH was decreased to 3.0 by adding HCl (6M) to facilitate flocculation of

the delaminated solid, which was recovered by centrifugation. After being washed with distilled water and dried at 60 °C for 12 h, the solid was treated at 540 °C, first in N_2 for 3 h and then in air for 6 h. After this calcination treatment, all of the organics were decomposed, yielding a material with the structural and textural characteristics of ITQ-2.

2.2. Ti grafting process

After the two supports (MCM-41 and ITQ-2) were calcined, a grafting process on the silicate surfaces was performed [16], using dichlorotitanocene (Aldrich, 97 wt%) as the Ti precursor. First, the samples were dried at 150 °C under vacuum. After cooling to room temperature, the selected quantity of TiCl_2Cp_2 solution (10 wt%) in chloroform (Aldrich, 99.5 wt%) was dosed to graft Ti onto the support surface, and then chloroform was added until a liquid/solid nominal ratio of 10 was achieved. This mixture was maintained under agitation for 1 h. Then a solution of triethylamine (Scharlau, extra-pure) in chloroform (molar ratio of $\text{NET}_3/\text{TiCl}_2\text{Cp}_2 = 2$) was used to activate the silanol groups of the supports and favor Ti grafting, with the mixture maintained under agitation for 1 h at room temperature. The suspensions were then filtered, washed with dichloromethane, and dried at 60 °C. A second calcination was performed at 540 °C to remove the cyclopentadienyl ligands. Six different Ti contents for each support were selected for the grafting process; the theoretical levels were 0.1, 0.5, 1, 2, 3, and 5 wt% $\text{TiO}_2/\text{SiO}_2$. Fig. S2 in Supplementary material shows the XRD patterns for the supports (MCM-41 and ITQ-2) after the Ti grafting process with different Ti ratios, which demonstrate no appreciable differences in structure after the treatment.

2.3. Silylation of the catalysts

Once the samples were dried at 150 °C under vacuum and cooled to room temperature, a solution with the proper quantity of the selected hexaalkyldisilazane in toluene (wt% toluene/silica = 10) was added. The corresponding synthesis mixture was maintained under reflux for 1 h at 85 °C. Then the rack was washed and filtered with toluene and dichloromethane, and the samples were finally dried at 60 °C. Four silylating agents were used: 1,1,1,3,3,3-hexamethyldisilazane (Aldrich), 1,3-dibutyl-1,1,3,3-tetramethyldisilazane (ABCR), 1,3-diphenyl-1,1,3,3-tetramethyldisilazane (ABCR), and 1,1,3,3-tetraphenyldimethyldisilazane (ABCR) (see Table S1 in Supplementary material). Six theoretical $\text{SiR}_3/\text{SiO}_2$ molar ratios were selected for both the MCM-41 support (0.05, 0.1, 0.15, 0.2, 0.5, and 1 $\text{SiR}_3/\text{SiO}_2$) and the ITQ-2 support (0.03, 0.06, 0.11, 0.3, 0.4, 0.5 $\text{SiR}_3/\text{SiO}_2$).

2.4. Catalytic testing

The solvent-free epoxidation of 4-decene (Aldrich >99%), with tert-butylhydroperoxide (TBHP; Aldrich, 80% in di-tert-butylperoxide/water 3/2) as the oxidant, was carried out in 2-mL glass flasks at 70 °C under magnetic stirring, using an olefin/oxidant molar ratio of 4 and 15 mg of catalyst per mL of feed. Aliquots were analyzed at different reaction times by gas chromatography (HP-5 column), and products were identified by mass spectroscopy. Response factors of the different compounds were determined to accurately calculate the conversion and selectivity of the process.

Epoxidation of methyl oleate was done in 1,3,5-trimethylbenzene as the solvent, with the following molar composition of the feed: 67.6% 1,3,5-trimethylbenzene, 23.2% methyl oleate, 5.8% tert-butylhydroperoxide, 0.5% di-tert-butylperoxide, and 2.9% H_2O . The reaction was performed at 30 °C using 5 mg of catalyst per mL of feed. Because of the high boiling point of methyl oleate and the

reaction products, an on-column injection mode was used for the chromatographic analysis. Calculation of conversion and selectivity levels was performed as done for 4-decene.

2.5. Catalyst characterization

Powder X-ray diffractometry (XRD) was performed with a HT Philips X'Pert MPD diffractometer equipped with a PW3050 goniometer using $\text{CuK}\alpha$ radiation and a multisample handler. DR UV–vis spectra were obtained with a Perkin Elmer (Lambda 19) spectrometer equipped with an integrating sphere with BaSO_4 as a reference. Concentrations of Ti were determined by atomic absorption, using a Varian SPECTRAA-10 plus. Thermogravimetric (TG) analysis was performed with a Mettler Toledo TGA/SDATA851e between 20 and 800 °C, with the loss of weight up to 150 °C assigned to water adsorbed on the surface of the samples. Elemental analysis was done with a Carlo Erba 1106 analyzer.

2.6. Description of high-throughput equipment

To reduce the experimental effort, various high-throughput (HT) equipment was used (Fig. S3 in Supplementary material). A Sophas automated robotic system (Zinsser Analytic) was used for grafting Ti and silylating the titanosilicates. Initially, solutions containing a proper concentration of reagents (Ti precursor and silylating agents) were placed into different containers, with pure silica ITQ-2 and MCM-41 distributed in a multivial rack. The addition of accurate amounts of each solution, as described previously, was done automatically using a multichannel syringe that can operate under nitrogen atmosphere. Samples were simultaneously heated and stirred (vortex system) in the corresponding station and washed and filtered using filtration probes (Zinsser Analytic) for the robotic system. These special tips can be used to either filter liquid from a liquid–solid mixture or to wash a solid, thanks to a central channel with a filter and two additional coaxial channels for the delivery/aspiration of gases or solvents. In our case, washing of the samples after the Ti grafting and silylation process was done by successive additions/extractions of the selected solvent (toluene or dichloromethane), using the aforementioned filtration probe.

HT catalytic testing was performed in an in-house-built system that allows parallel processing of 21 batch reactions independently stirred (500 rpm) and heated by a temperature-controlled aluminum rack. No mass transfer limitations were detected at >300 rpm when the stirring rate was varied from 0 to 700 rpm. A programmable autosampler was used to sequentially obtain aliquots from the different reactors, and the samples were analyzed in a coupled online GC. Data acquisition and calculations were performed in real time as results were obtained from each reactor. As reported previously [10], epoxidation experiments using this robotic system are both reproducible and scalable.

3. Results and discussion

3.1. First factorial design of catalysts and physicochemical characteristics of titanosilicates silylated with SiMe_3

The present work was undertaken to study the behavior of epoxidation catalysts consisting of Ti species grafted on structural silicates whose surface was modified by a silylating agent (SiR_3). Let us initially suppose that one unique type of modifier must be evaluated, with the effects of Ti and SiR_3 on the catalyst activity analyzed. In this simple case, the activity of the material for a specific reaction becomes a simple function of the nominal Ti and SiR_3 content, and the best Ti– SiR_3 combination can be readily identified through a factorial design of experiments. For instance, we

Table 1

Factorial design for each support (MCM-41 and ITQ-2) using SiMe_3 as silylating agent (36 samples for each one), together with selected samples for full characterization

	Theoretical $\text{TiO}_2/\text{SiO}_2$ (wt%)						
	0.1	0.5	1	2	3		5
Theoretical SiMe_3 (molar ratio)	0.03	×	×	×	×	0.05	Theoretical SiMe_3 (molar ratio)
	0.06					0.1	
	0.11					0.15	
	0.3	×	×	×	×	0.2	
ITQ-2	0.4					0.5	MCM-41
	0.5		×	×	×	1	

×, TGA and elemental analysis.

first evaluated the response of Ti-MCM-41, and Ti-ITQ-2 catalysts modified with a unique silylating agent (SiMe_3) on the epoxidation of 4-decene (test reaction), using the full factorial design shown in Table 1 (36 samples per support). Thanks to an homogeneous distribution of experiments along the space of research, a general overview of the catalytic response for both materials can be provided (Fig. 1), indicating that activity, measured as initial reaction rate, reaches maximum values at certain levels of Ti and SiMe_3 (distance weighted least squares was used to generate the surfaces in Fig. 1).

It can be seen that the catalyst activity increases rapidly with Ti content up to a nominal $\text{TiO}_2/\text{SiO}_2$ % weight ratio of 2–3 and remains nearly constant or even decreases slightly for higher values. Measurement of the actual Ti content in the samples by absorption spectroscopy shows that only insignificant differences between the nominal and actual loadings (Table S2 in Supplementary material), indicating that within the range studied in this work, all of the Ti species can be easily grafted onto MCM-41 and ITQ-2 supports. Nevertheless, UV–vis spectroscopy of catalysts with increasing metal content (Fig. 2) shows that partial polymerization of Ti occurs above 2 wt% $\text{TiO}_2/\text{SiO}_2$ on both materials, as can be inferred by the presence of a prominent signal in the 250–300 nm region. Taking into account the poor activity of these nontetrahedrally coordinated Ti species in epoxidation reactions [17], a slight decrease in the initial reaction rate would be expected at high Ti content, as is shown in Fig. 1.

Elemental analysis of samples with different theoretical amounts of silylating agents (see Table 1) was done to evaluate the effectiveness of the anchoring process. Taking into account the percentage of carbon present in the catalysts, the actual $\text{SiMe}_3/\text{SiO}_2$ molar ratio was calculated and is plotted against the nominal values in Fig. 3. For both MCM-41 and ITQ-2, the maximum amount of SiMe_3 molecules fixed onto the silicate surfaces is much lower than the maximum nominal value derived from the silanol capacity and the monolayer value; therefore, the asymptotical variation of activity with the theoretical $\text{SiMe}_3/\text{SiO}_2$ ratio (Fig. 1) could be related to the achievement of maximum hydrophobicity due to the silylation. MCM-41, with a higher external surface than ITQ-2 (~900 vs 750 m^2/g), has a maximum $\text{SiMe}_3/\text{SiO}_2$ molar ratio of 0.19, which is superior to the 0.17 value found for ITQ-2. As expected, the previous grafting of Ti onto the support also affects to the effectiveness of the silylation process (Fig. 3, dotted line), even though the differences are relatively small compared with the direct effect of the nominal SiMe_3 amount. Complementarily, TGA of silylated Ti-ITQ-2 and Ti-MCM-41 was carried out to estimate the hydrophobicity of the catalysts, assuming that the greater the water content, the less hydrophobic the sample.

In the absence of surface modifier and Ti species, ITQ-2 is more hydrophilic than MCM-41 (water loss, 11.5 vs 8.5 wt%). Fig. 4 shows a very significant influence of SiMe_3 level on hydrophobicity at lower surface coverage of the silylating agent, with much less water loss on heating at higher degrees of silylation. It can be seen

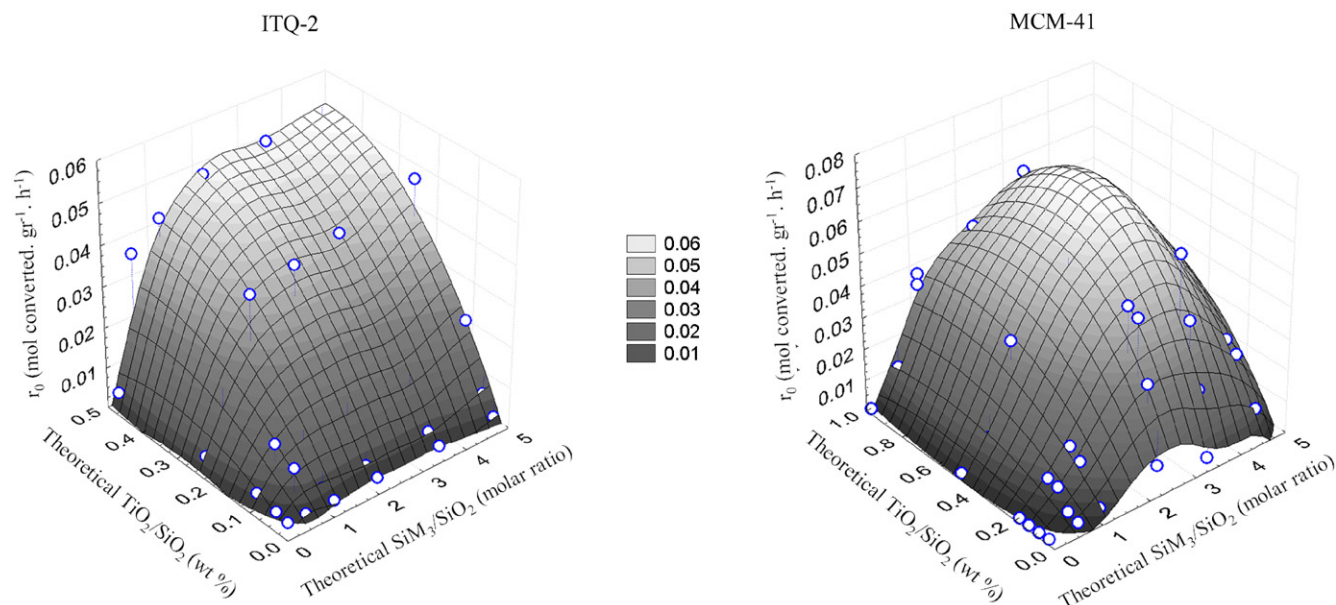


Fig. 1. Modeling of catalysts response as a function of the theoretical Ti and SiMe₃ contents.

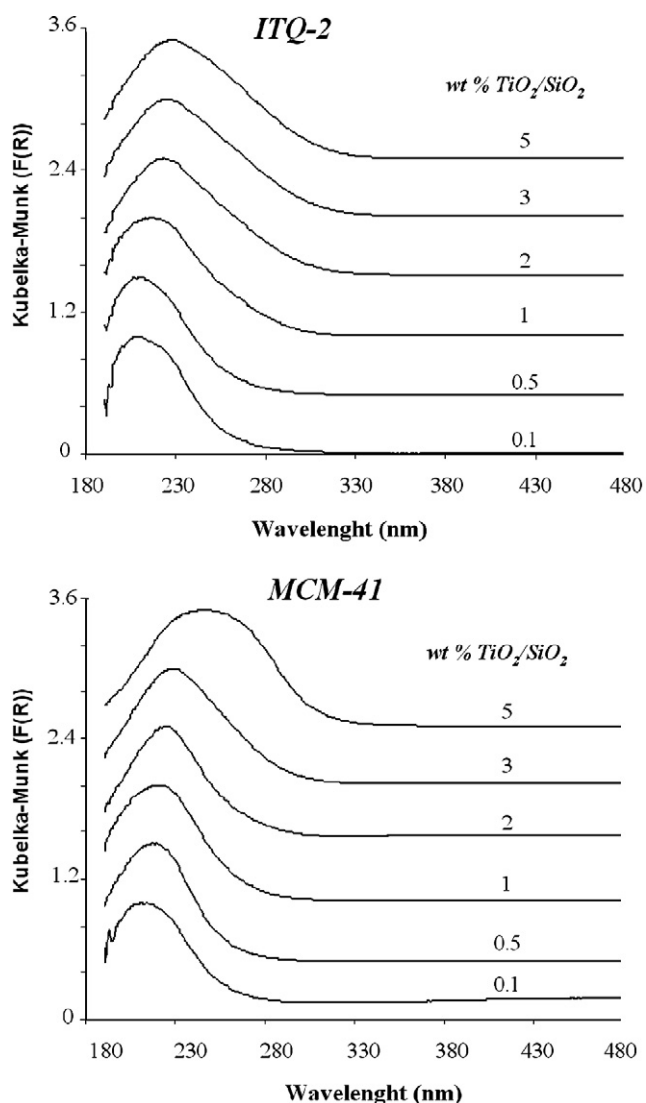


Fig. 2. UV-vis DRS spectra for the Ti-MCM-41 (top) and Ti-ITQ-2 (bottom) samples before the silylating process.

that the maximum level of hydrophobicity occurs slightly before the surface of the support is saturated with SiMe₃ groups.

Interestingly, the presence of Ti grafted on the supports has an influence on the physical-chemical properties of the catalyst. The hydrophobicity of the samples increases with increasing Ti content at the same degree of silylation.

3.2. Advanced strategies in the exploration of new research spaces

3.2.1. Examination of existing strategies

In the previous section we discussed the effect of Ti and silylating agent content on the catalytic behavior (4-decene epoxidation as test reaction) of the MCM-41 and ITQ-2 catalysts with SiMe₃ used as a surface modifier. But the estimated correlations (smoothed surfaces in Fig. 1 for ITQ-2 and MCM-41) are valid only when SiMe₃ is used as a silylating agent. Predicting the activity of new catalysts based on different surface modifiers obviously will require more experiments. Despite the fact that data from the SiMe₃ space on both MCM-41 and ITQ-2 suggest that highest activities are found at nominal TiO₂/SiO₂ values (% weight ratio) near 3 and when using an excess of SiR₃ during silylation of the supports, the development of a complete map of activity able to estimate the influence of these two variables for the entire space of study (i.e., all silylating agents) is of interest for two reasons (a) An accurate map will provide valuable fundamental knowledge about the mode of action of the surface modifiers, on adsorption-interaction of reactants and products, and (b) an overview of the study will help determine the maximum activity for each silylating agent and also establish the optimal synthesis conditions that avoid unnecessary excesses of reagents (Ti and SiR₃). Consequently, we evaluated the effect of Ti and SiR₃ content on the catalytic behavior of ITQ-2 and of MCM-41 modified by other silylating agents (SiMe₂Ph, SiMe₂Bu, and SiMePh₂), again using 4-decene epoxidation as the test reaction. In this situation, a traditional approach involves duplicating the previous experimental plan on the SiMe₃ modifier for each one of the new SiR₃; however, we believe that this strategy, although relatively simple, can be improved in terms of both the effort required and the quality of the estimated maps.

Some advanced strategies for minimizing the number of experiments when different but closely related systems must be consecutively evaluated have been proposed in the literature [18]. It has been proposed that neural networks (NNs) [19,20] and support

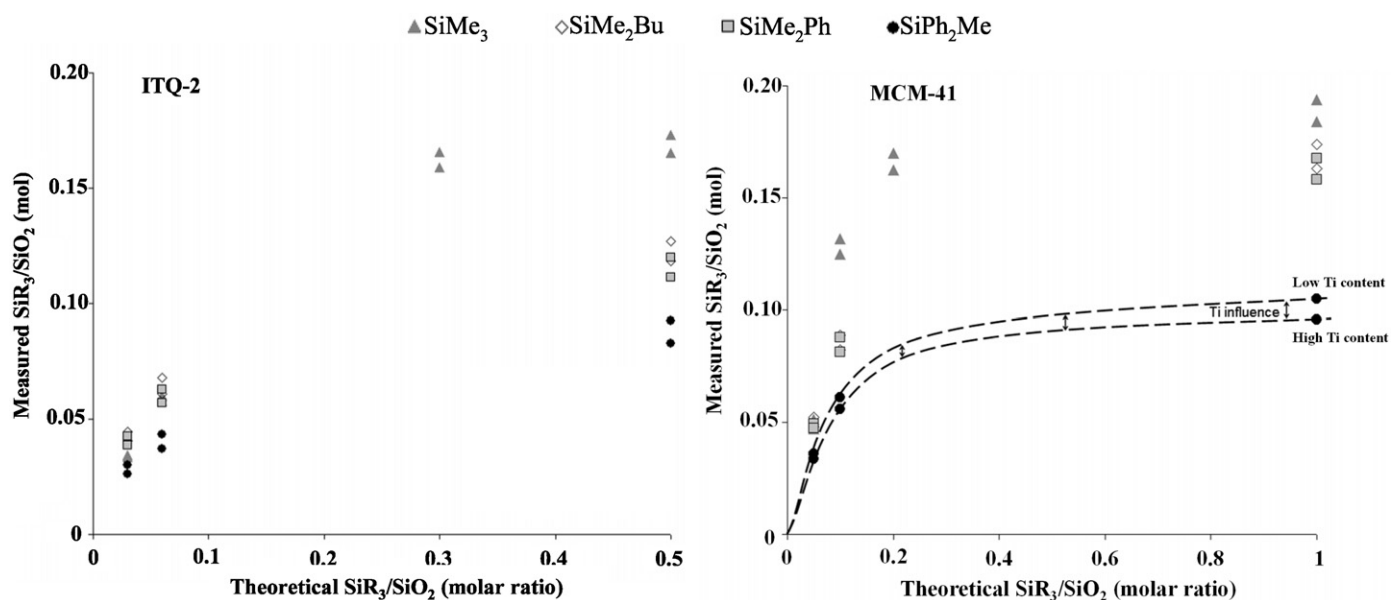


Fig. 3. Real amounts of SiR_3 agents anchored onto the ITQ-2 and MCM-41 surfaces (calculated from elemental analysis of the samples) for different nominal $\text{SiR}_3/\text{SiO}_2$ ratios. See Table 2 for experimental design. For a given amount of theoretical $\text{SiR}_3/\text{SiO}_2$, two catalysts with two different levels of Ti have been characterized as specified in Table 2. For each vertical pair of points considering one given silylating agent, the upper point corresponds to the catalyst on which fewer Ti atoms have been grafted.

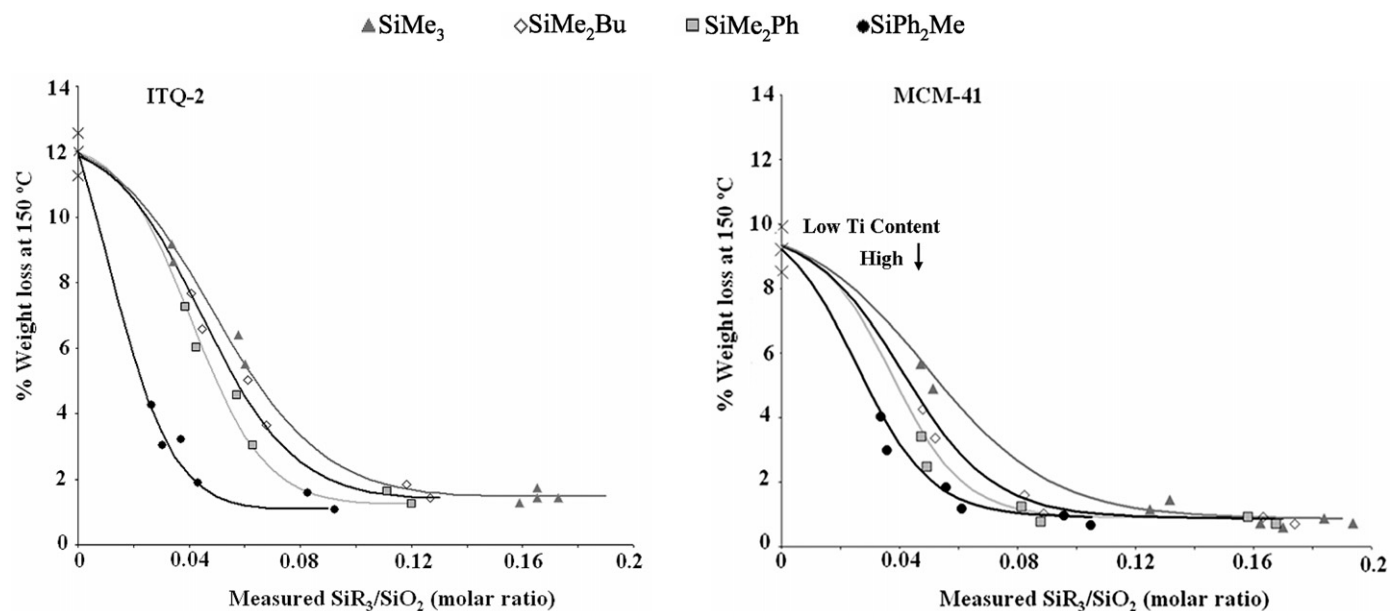


Fig. 4. Results of the thermogravimetric analysis of samples with increasing contents of surface modifiers. See Table 2 for experimental design. Crosses on the y-axis (\times) are nonsilylated catalysts with different levels of Ti. The presence of Ti grafted on the supports has an influence on the physical–chemical properties of the catalyst, and the hydrophobicity of the samples, at the same silylation degree, increases when increasing the Ti content.

vector machines (SVMs) [21] can reduce the experimental effort by means of *in silico* evaluations, once the model has been properly trained by a certain number of real data. Indeed, it has been shown that NNs can “learn” about one space of research (i.e., the reactivity of one molecule) and then build a mathematical model whose structure also can be applied in a similar but slightly different research space (i.e., the behavior of a related molecule in the same type of reaction) [22]. But a critical analysis is frequently performed by more fundamental chemists, who accept the practical contribution of such innovative strategies but reject the use of black box tools, which provide little chemical insight and are difficult to understand. Consequently, we decided to develop an alternative strategy involving the use of an advanced modeling tool to reduce the experimental effort and allow the retrieval and

use of fundamental information. Essentially, this methodology is based on introducing useful chemical information about the textural properties of the catalysts into an NN. Using this approach, we attempt to use the findings of a few real experiments to predict the entire Ti– SiR_3 map, similar to that shown in Fig. 1 for SiMe_3 , but using other surface modifiers, such as SiMe_2Ph , SiMe_2Bu , and SiMePh_2 .

3.2.2. Molecular modeling and characterization

First, we selected six samples for each of the new silylating agents (Table 2; note that one of the cross-shaped marks actually corresponds to a nonsilylated sample) to be experimentally evaluated (i.e., synthesized, characterized, and tested for 4-decene epoxidation). The characterization of such catalysts by elemental

analysis and TGA allows the production of new curves in Figs. 3 and 4. It can be seen that the use of surface modifiers more voluminous than SiMe_3 leads to a reduction in the maximum amount of silylating agents that can be anchored onto the surface of the supports. This suggests increasing sterical constraints among nearby molecules with increasing SiR_3 . Moreover, slight differences also are seen in the TGA results, with the samples silylated with the smallest amounts of SiR_3 demonstrating the least hydrophobicity at a given surface $\text{SiR}_3/\text{SiO}_2$ ratio. Interestingly, SiMe_2Bu and SiMe_2Ph , with similar effective molecular dimensions, show very similar elemental analysis and TGA results. The grafting of Ti onto the supports before fixing the silylating agents, although affecting the results, is of minor significance (Figs. 3 and 4).

After the characterization and proper modeling of the new catalysts, we worked on integrating knowledge of the chemical properties of the different SiR_3 , taking into account that to evaluate their mode of action from a chemical standpoint, we need to be able to transform simple qualitative objects (silylating agent A, B, C, or D) into well-defined entities. Thus, we considered various molecular descriptors, including constitutional information (atomic Sanderson electro-negativities, atomic polarizabilities, electro-topological state, aromatic ratio, and number of bonds that can rotate); geometrical information (average geometric distance degree, spin ratio, sphericity, asphericity, Petitjean shapes, and aromaticity); and molecular properties (unsaturated index, and hydrophilic factor), to establish the main chemical properties of the silylating agents (see Ref. [23] for related terminology). These properties were calculated for the different silylating agents using Dragon software [24].

Table 2
Experimental design for characterization of SiMe_2Bu , SiMe_2Ph , and SiMePh_2

	Theoretical $\text{TiO}_2/\text{SiO}_2$ (wt%)						
	0.1	0.5	1	2	3	5	
Theoretical SiR_3^a	0			×		0	Theoretical SiR_3^a
(molar ratio)	0.03	×		×		0.05	(molar ratio)
	0.06			×	×	0.1	
	0.11					0.15	
ITQ-2	0.3					0.2	MCM-41
	0.4					0.5	
	0.5		×		×	1	

×, TGA and elemental analysis (carbon).

^a R = { Me_2Bu ; Me_2Ph ; MePh_2 }.

3.2.3. Enhanced predicting tools by fundamental knowledge integration

We selected NNs to model the catalytic data in the present work. These models involve advanced predicting algorithms that are able to search for complex mathematical relationships between some inputs (e.g., variables to define a group of catalysts) and some outputs (e.g., variables to define their catalytic response). Compared with other traditional modeling tools, NNs can be distinguished due to their particular mathematical definition, in which the influence of each input variable on the final response (output variable) is weighed through consecutive nonlinear relationships (see Supplementary material). To find the best way to link the information, NNs must be previously calibrated to fit their internal parameters (so-called training step), similarly to the fitting process performed with any other type of mathematical model. Because NNs can easily adapt to nonlinear spaces by simply increasing the model complexity, it is always important to be sure that the predicted responses are really representative of the problem (avoiding the so-called overfitting of the NN). Thus, a special fitting procedure (so-called cross-validation) is usually performed, where part of the known data is used to calibrate the parameters of the model, while the rest is used to check the robustness of the response (see Supplementary material).

In the present work, information on the six samples studied for each SiMe_2Ph , SiMe_2Bu , and SiMePh_2 agent (reactivity, characterization, and molecular descriptors), together with information about all of the samples processed for the SiMe_3 (36 samples per support) were introduced as input variables into a very simple NN, to correlate their catalytic behavior (output variable) with the chemical aspects of the reaction (selection of NN architecture, fitting of parameters, validation step, etc.; see Supplementary material).

To clearly demonstrate that the integration of knowledge from characterization and molecular modeling does positively affect the quality of the prediction, we have compared the results provided by this methodology with a second one which does not integrate additional information. The alternative neural network was trained with data only containing information about the nominal Ti, nominal SiR_3 values (with the silylating agents represented as a qualitative variable), and catalytic results. Fig. 5 and Fig. S4 in Supplementary material show the estimated correlations for MCM-41 and ITQ-2 spaces (calculated vs experimental results) using both techniques. In addition to the samples used during the training of the neural networks, 12 new samples, which have not been used to train the algorithms, have been predicted and compared with

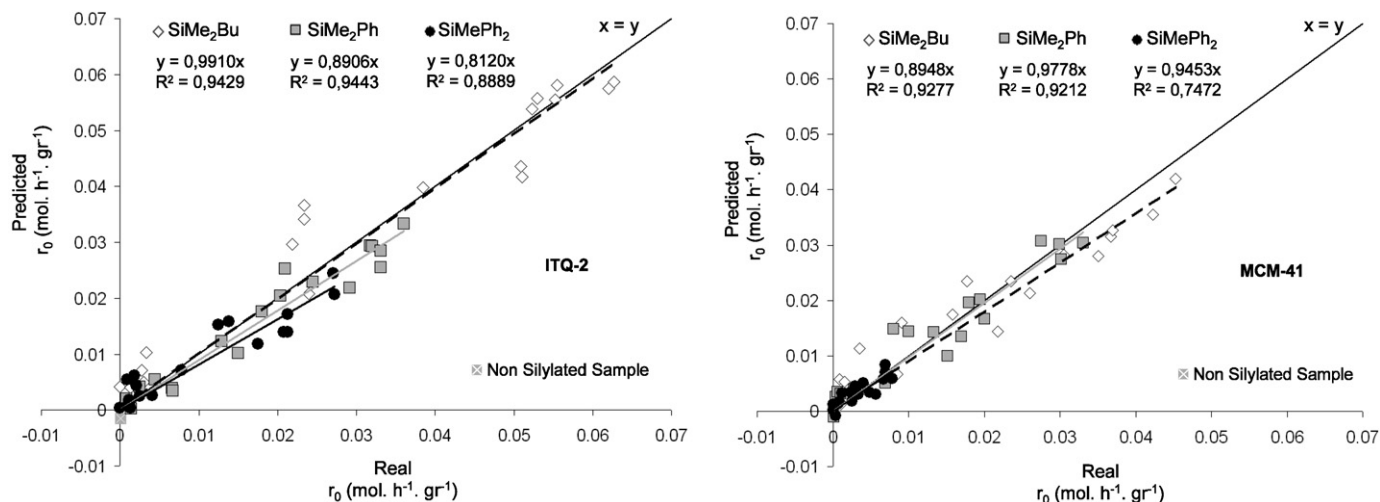


Fig. 5. Correlation between the initial reaction rate ($\text{mol converted h}^{-1} \text{g}^{-1}$) experimentally observed, and predicted by the neural network when characterization and molecular modeling are used to describe the synthesized catalysts.

Table 3

Catalytic results of the best catalysts for each type of support modified by the different silylating agents. According to the estimated maps of activity, TOF values can be maximized while keeping excellent levels of activity

Support	Silylating agent	TiO ₂ /SiO ₂ (wt%) ^a	SiR ₂ /SiO ₂ (molar ratio) ^a	r ₀ ^b	TOF (h ⁻¹)	% S ^c
ITQ-2	SiMe ₃	3	0.5	0.0486	106	97.8
	SiMe ₂ Bu	2	0.5	0.0623	221	97.5
	SiMe ₂ Ph	3	0.3	0.0331	71	97.2
	SiMePh ₂	3	0.5	0.0272	59	98.7
MCM-41	SiMe ₃	3	0.5	0.0577	152	99.2
	SiMe ₂ Bu	3	0.5	0.0458	81	97.5
	SiMe ₂ Ph	2	0.5	0.0330	130	97.3
	SiMePh ₂	3	1	0.0054	14	97.8
ITQ-2	SiMe ₃	0.5	0.4	0.0351	440	98.8
MCM-41	SiMe ₃	1	0.3	0.0305	250	99.3

Reaction conditions: solvent-free solution with a 4-decene/TBHP molar ratio = 4; 15 mg of catalyst per 1 mL of solution; T = 70 °C.

^a Nominal values.

^b Initial reaction rate as mol of epoxide per gram of catalyst and hour.

^c Measured at 40% conversion, excepts for MCM-41 modified by SiMePh₂ (20% conversion).

the experimental catalytic results in Fig. 5 and Fig. S4 in Supplementary material. It can be observed that the general level of error, measured as exactness (the closer the slope to 1, the better) and precision (the better the regression coefficient, the less the variance/noise) of the NN response is notably better when characterization and molecular descriptors data are introduced into the network (NN1). Using this model, and applying the correlations in Figs. 3 and 4 about experimental SiR₃/SiO₂ and TGA values, a reliable response surface of the different SiR₃ spaces can be predicted, allowing to extract the maximum levels of activity for each silylating agent (Fig. 5 and Table 3), and the best results can be obtained by minimizing the use of SiR₃ and Ti (Fig. S5 and Table 3). The algorithm shows that the industrially most commonly used silylating agent, SiMe₃, provides the highest activities for the MCM-41 material at relatively high Ti content (3 wt%), whereas the most flexible surface modifier, SiMe₂Bu, gives the best behavior for ITQ-2 samples. Moreover, it can be seen that by optimizing the use of Ti and surface modifier, TOF values of around 450 (mol converted per mol Ti and h) can be obtained with the Ti-ITQ-2/SiMe₃ system. This value is twice the intrinsic activity levels shown by MCM-41. Taking into account the prediction of initial reaction rates by the NN1 model, along with the measured Ti content of the different samples, we created a complete TOF map (Fig. S5 in Supplementary material), which shows that best TOFs are provided when SiMe₃ is used as the silylating agent, independent of the type of support. Along with initial reaction rates, Table 3 shows high selectivity and TOF values for the most active catalysts with each silylating agent. Moreover, taking into account that epoxidation catalysts are required to provide high yields from an industrial standpoint, we followed the evolution of conversion and selectivity with reaction time for the best Ti-ITQ-2 and Ti-MCM-41 materials (Fig. 6). We found that yields to 4-decene epoxide >70% can be obtained, indicating that deactivation, if it occurs, is not very strong. Thus, based on these observations, highly efficient epoxidation catalysts can be inferred as a result of a proper selection of supports (high external surface), proper loadings of Ti (well-dispersed Ti⁴⁺ species), and proper activation of Ti sites (protection by means of silylating agents).

On the other hand, we also carefully checked the NN1's behavior using the characterization, reactivity, and molecular modeling data. Fig. 7 shows the relative influence of the variables extracted by the NN. A feature selection algorithm [25] has been combined with the NN to identify input variables that do not contribute significantly to the network performance and remove them (so-

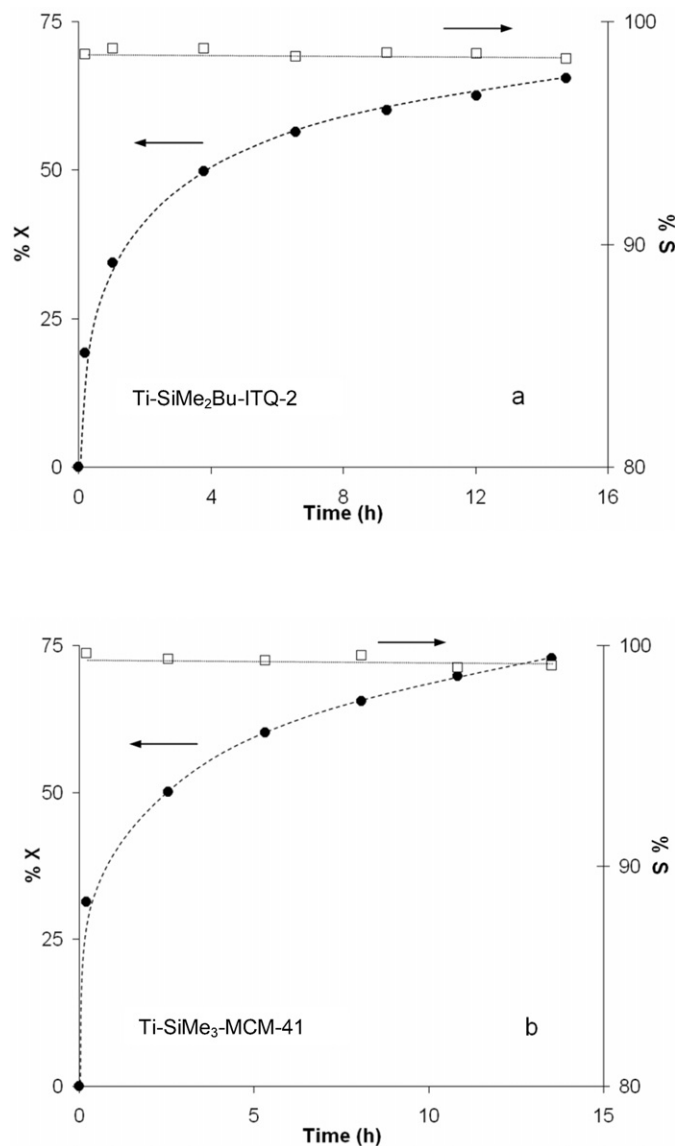


Fig. 6. Evolution of conversion and selectivity with reaction time with the best found Ti-ITQ-2 (a: 2 wt% TiO₂/SiO₂, 0.5 SiMe₂Bu/SiO₂ molar ratio) and Ti-MCM-41 (b: 3 wt% TiO₂/SiO₂, 0.5 SiMe₃/SiO₂ molar ratio) catalysts during the epoxidation of 4-decene.

called “pruning”). This approach allows us to discard overfitting [26] while achieving very simple network architectures (see Fig. S6 in Supplementary material).

As expected, Ti loading was found to be the most important factor for both the ITQ-2 and MCM-41 supports. Moreover, relevant differences in terms of the nature of the silylating agent were found. For the MCM-41 support, the volume occupied by the SiR₃ molecules was found to be the second major factor. This seems logical considering that the wall of the mesoporous material behaves as an extensive “external surface” with homogeneous Si–OH groups along the channels. In contrast, the ITQ-2 material exhibited a wide heterogeneity of external silanols due to numerous structural defects on different structural positions [27]. Consequently, another factor related to the flexibility of the silylating agent is relevant for efficiently protecting the Ti active sites. For this reason, even if SiMe₂Bu and SiMe₂Ph present similar molecular dimensions (as well as similar results for elemental and TG analyses), poor levels of activity are obtained by silylating with the more rigid SiMe₂Ph agent.

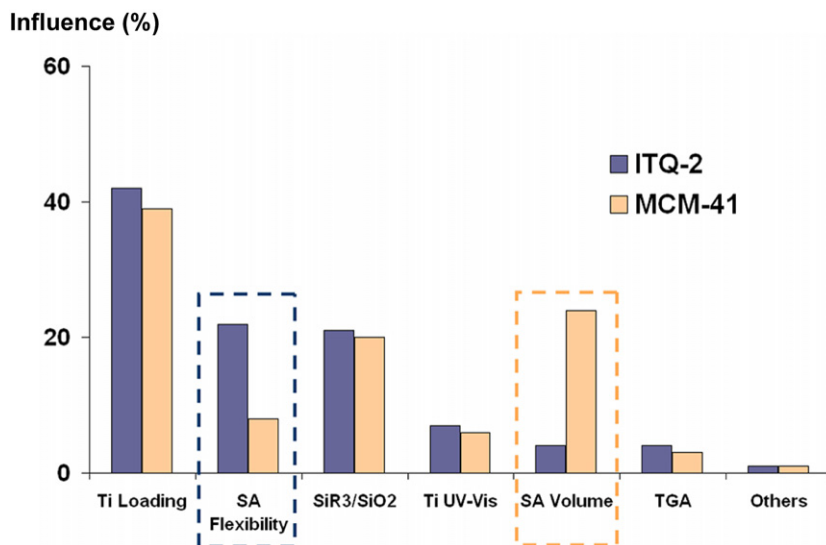


Fig. 7. Estimation provided by the neural network on the relative influence of the ITQ-2 and MCM-41 properties in their catalytic behavior.

Our modeling also establishes that TGA, which measures the amount of water adsorbed by the samples, is not the only factor that should be considered when correlating the catalyst activity. In fact, although we found that more voluminous silylating agents generated higher general levels of hydrophobicity (Fig. 4), the use of SiMePh₂ provided very low activity for both MCM-41 and ITQ-2. Then another factor (i.e., real SiR₃/SiO₂ ratio), which is related to the number of remaining free OH groups after silylation, is also an important factor in the activity of the samples (see Fig. 7). From this standpoint, it can be inferred that when small surface modifiers are used and less free OH remains at a certain silylation degree, more efficient Ti environments are produced, leading to high levels of activity.

3.3. Using test reactions with model molecules to predict the behavior of industrial feeds

After completing the preliminary study with 4-decene as a model reactant, we finally evaluated the behavior of some Ti-ITQ-2 and Ti-MCM-41 catalysts on the epoxidation of a more industrially relevant substrate, methyl oleate. We expected to see a correlation between the 4-decene and methyl oleate results and to find that 4-decene could be used to predict the complete response of the catalysts in the methyl oleate space (i.e., of Ti and SiR₃ content, type of silylating agent, and support) with a greatly number of experiments. Based on this hypothesis, we tested only 11 samples for ITQ-2 and MCM-41, covering the different types of surface modifiers and a wide range of activity levels, for the epoxidation of methyl oleate. (Reaction conditions were adapted to the high reactivity of this molecule to accurately calculate initial reaction rates.) Note that no special strategy was used to select these 22 experiments (11 per support); the criterion was simply diversity along the initial reaction rate according to the 4-decene results.

Results on the activity of these catalysts for the epoxidation of methyl oleate were then plotted versus those obtained in the epoxidation of 4-decene (Fig. 8a), with selectivity to the epoxide of all tested samples >98%. A certain linear correlation between the activities of the catalysts with both reagents can be seen (Fig. 8a), even though a very poor regression coefficient was obtained for Ti-ITQ-2. It also can be seen that Ti-ITQ-2 generally was more active than Ti-MCM-41 in epoxidation of the fatty ester, as can be inferred from the higher slope of the former in Fig. 8a. We can then hypothesize that the zeolitic structure of Ti-ITQ-2 is better suited for reacting this olefin than the mesoporous structure of

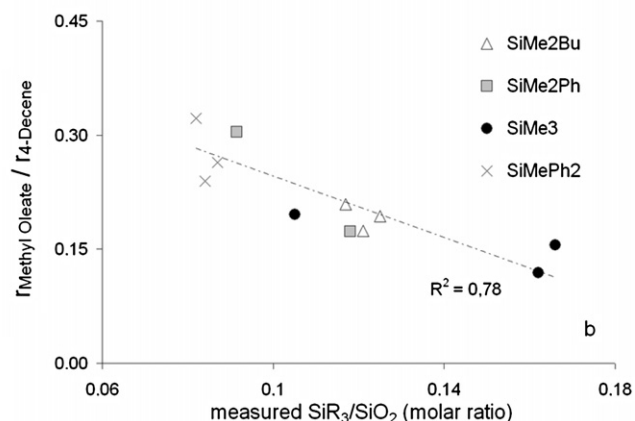
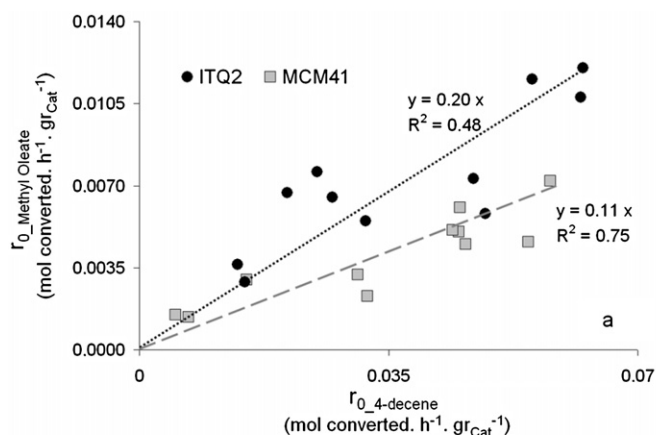


Fig. 8. (a) Correlation between the activity of ITQ-2 and MCM-41 samples for the 4-decene and the methyl oleate substrates. (b) The quality of the fitness for the ITQ support can be improved by taking into account a measure of the hydrophobicity of the catalysts.

MCM-41, due to a more favorable coupling between the nature of the reactant and the support. Note that even though we cannot disregard the fact that different reaction conditions were used (solvent-free, 70 °C, and 15 mg per mL of feeding for 4-decene; 1,3,5-trimethylbenzene as solvent, 30 °C, and 5 mg per mL of feed-

ing fir methyl oleate) to accurately calculate the corresponding initial reaction rates, we believe that the different structural configurations of the supports (short-range crystalline for ITQ-2 and amorphous for MCM-41) has an important effect on the adsorption/activation properties of the alkene. Indeed, taking into account the different polarities of 4-decene and methyl oleate (which contains a more polar ester group), the higher hydrophilicity of ITQ-2, as shown in the TGA of nonsilylated materials, should be more than adequate to activate the more polar substrate. On the other hand, the poor correlation between the ITQ-2 samples ($r_{4\text{-decene}}$ vs $r_{\text{methyl oleate}}$, $R^2 = 0.48$) shown in Fig. 8a suggests that some other catalytic factor affects the epoxidation of the two substrates in a slightly different manner. After checking different possibilities for obtaining more accurate but still simple relationships (see Fig. S7 in Supplementary material), we found that when the measured molar $\text{SiR}_3/\text{SiO}_2$ ratios are taken into account, a new, improved correlation to link 4-decene and methyl oleate spaces can be found (Fig. 8b, $R^2 = 0.78$). Moreover, the resulting linear decrease in the $r_{\text{methyl oleate}}/r_{4\text{-decene}}$ ratio with increasing molar $\text{SiR}_3/\text{SiO}_2$ ratio (Fig. 8b) confirms the hypothesis that more hydrophobic surfaces are actually less favorable for more polar substrates. Interestingly, as was suggested by NN1, the experimentally determined SiR_3 content was found to be more representative than TGA values for evaluating the true hydrophobicity of Ti environments, as can be inferred by the poor $r_{\text{methyl oleate}}/r_{4\text{-decene}}$ correlation obtained when this latter parameter was considered (Fig. S7 in Supplementary material).

On the other hand, it is important to stress that both correlations in Figs. 8a and 8b are independent of the type of silylating agent, because they exhibit simple linear trends based on few catalysts per surface modifier. Therefore, we can assume that, with a relatively low margin of error, 4-decene epoxidation can provide a trustable test reaction for evaluating a more relevant industrial case, such as methyl oleate epoxidation.

We found that maximum initial reaction rates for methyl oleate epoxidation were provided by the Ti-ITQ-2 samples silylated by SiMe_2Bu . This may be due to the high flexibility of this modifier, which offers effective protection of Ti sites onto the irregular ITQ-2 surface while still leaving free external OH^- , which is crucial for proper activation of methyl oleate. In contrast, the most commonly used SiMe_3 modifier on the zeolitic material, even when providing high initial reaction rates with 4-decene, leads to quite low levels of activity for epoxidation of the fatty ester. In any case, when conversion and selectivity levels for the most active Ti-ITQ-2 and Ti-MCM-41 catalysts are plotted versus reaction time (Fig. 9), it can be seen that high yields of epoxide again are provided. The fact that such a voluminous surface modifier can be effectively used even for such a large amount of reactant suggests that there are no limitations to the accessibility to the Ti active sites during the reaction.

4. Conclusion

A new strategy that combines advanced technologies, such as high-throughput experimentation, molecular modeling, and advanced data-mining tools, with the traditional catalyst development (fundamental knowledge and characterization) has been successfully used to optimize the catalytic behavior of two ordered titanasilicate materials for the epoxidation of large olefins. Such a methodology not only reduces the experimental effort, but also facilitates information retrieval and provides insight into the roles of the different catalyst variables. In this sense, a common black box algorithm, such as NN, is transformed into a valuable tool for automatically identifying chemical aspects of the process.

Although the use of surface modifiers is seen to notably enhance the activity of the samples while maintaining excellent

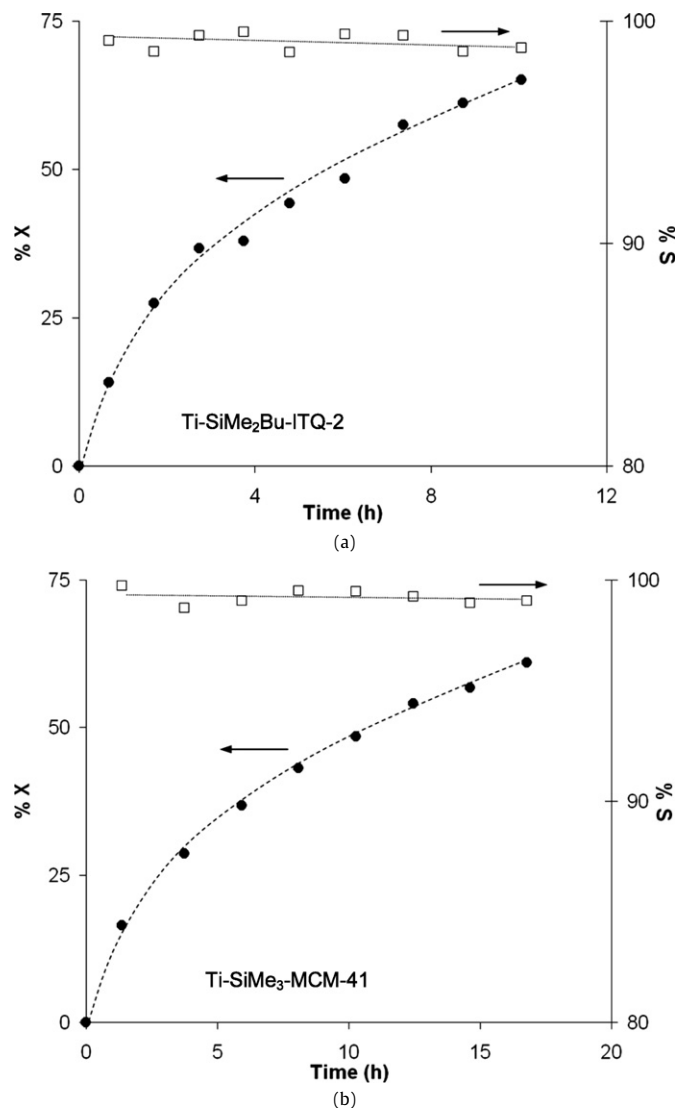


Fig. 9. Evolution of conversion and selectivity with reaction time with the best found Ti-ITQ-2 (a: 2 wt% $\text{TiO}_2/\text{SiO}_2$, 0.5 $\text{SiMe}_2\text{Bu}/\text{SiO}_2$ molar ratio) and Ti-MCM-41 (b: 3 wt% $\text{TiO}_2/\text{SiO}_2$, 0.5 $\text{SiMe}_3/\text{SiO}_2$ molar ratio) catalysts during the epoxidation of methyl oleate.

selectivity levels, it has been established that the support structure (more specifically, the surface properties) must be considered when dealing with each specific substrate. Our final results demonstrate that using flexible silylating agents, such as SiMe_2Bu , on delaminated zeolitic structures, such as ITQ-2, provides the optimum level of activity for the epoxidation of methyl oleate, thanks to the effective protection of the Ti environment in the presence of water and proper control of the hydrophobicity/hydrophilicity of the support. In contrast, SiMe_2Bu is not the most ideal silylating agent for Ti-MCM-41 for the epoxidation of methyl oleate due to the differing hydrophilicity of the two silicates.

Acknowledgments

This work was supported by EU Commission FP6 (TOPCOMBI Project [28]) and MAT 2006-14274-C02-01. The authors thank Santiago Jimenez for his scientific collaboration on the hiT_eQ platform that supports our calculations and Isabel Millet for technical support.

Supplementary material

The online version of this article contains additional supplementary material.

Please visit DOI: [10.1016/j.jcat.2008.05.033](https://doi.org/10.1016/j.jcat.2008.05.033).

References

- [1] (a) G.W. Huber, A. Corma, *Angew. Chem. Int. Ed.* **46** (2007) 7184;
(b) J.N. Chheda, G.W. Huber, J.A. Dumesic, *Angew. Chem. Int. Ed.* **46** (2007) 7164;
(c) A. Corma, S. Iborra, A. Velty, *Chem. Rev.* **107** (2007) 2411.
- [2] (a) G.W. Huber, P. O'Connor, A. Corma, *App. Catal. A* **329** (2007) 120;
(b) M. Stumborg, A. Wong, E. Hogan, *Bioresour. Technol.* **56** (1996) 13.
- [3] (a) S.K. Spear, S.T. Griffin, K.S. Granger, J.G. Huddleston, R.D. Rogers, *Green Chem.* **9** (2007) 1008;
(b) D. Kusdiana, S. Saka, *Bioresour. Technol.* **91** (2003) 289.
- [4] N. Prileschajew, *Ber. Dtsch. Chem. Ges.* **42** (1909) 4811.
- [5] U. Biermann, W. Friedt, S. Lang, W. Lühs, G. Machmüller, J.O. Metzger, M.R. Klaas, H.J. Schafer, M.P. Scheneider, *Angew. Chem. Int. Ed.* **39** (2000) 2206.
- [6] (a) F. Wattimena, H.P. Wulff, G.B. Patent 1249079 (1971), to Shell Oil Company;
(b) R. Millini, E.P. Massara, G. Perego, G. Bellussi, *J. Catal.* **137** (1992) 497;
(c) P. Ingallina, M.G. Clerici, L. Rossi, G. Bellussi, *Stud. Surf. Sci. Catal.* **92** (1995) 31;
(d) A. Thangaraj, R. Kumar, P. Ratnasamy, *J. Catal.* **131** (1991) 294.
- [7] (a) T. Blasco, A. Corma, M.T. Navarro, J. Perez-Pariente, *J. Catal.* **156** (1995) 65;
(b) W. Fan, P. Wu, S. Namba, T. Tatsumi, *J. Catal.* **243** (2006) 183;
(c) A. Corma, U. Díaz, M.E. Domine, V. Fornés, *J. Am. Chem. Soc.* **122** (2000) 2804;
(d) M.A. Camblor, M. Costantini, A. Corma, L. Gilbert, P. Esteve, A. Martínez, S. Valencia, *Chem. Commun.* **11** (1996) 1339;
(e) P. Wu, Y. Liu, M. He, T. Tatsumi, *J. Catal.* **228** (2004) 183.
- [8] (a) L.A. Ríos, P. Weckes, H. Schuster, W.F. Hoelderich, *J. Catal.* **232** (2005) 19;
(b) T. Blasco, M.A. Camblor, A. Corma, J. Perez-Pariente, *J. Am. Chem. Soc.* **115** (1993) 11806.
- [9] A. Corma, M.E. Domine, J.A. Gaona, J.L. Jordá, M.T. Navarro, F. Rey, J. Perez-Pariente, J. Tsuji, B. McCulloch, L.T. Nemeth, *Chem. Commun.* (1998) 2211.
- [10] (a) P.P. Pescarmona, K.P.F. Janssen, P.A. Jacobs, *Chem. Eur. J.* **13** (2007) 6562;
(b) P.P. Pescarmona, J.C. van der Waal, I.E. Maxwell, T. Maschmeyer, *Angew. Chem. Int. Ed.* **40** (2001) 743;
(c) T. Miyazaki, S. Ozturk, I. Onal, S. Senkan, *Catal. Today* **81** (2003) 473;
(d) A. Corma, J.M. Serra, P. Serna, E. Argente, S. Valero, V. Botti, *J. Catal.* **229** (2005) 513.
- [11] (a) M. Moliner, J.M. Serra, A. Corma, E. Argente, S. Valero, V. Botti, *Microporous Mesoporous Mater.* **78** (2005) 73;
(b) A. Corma, M.J. Díaz-Cabañas, J.L. Jordá, C. Martínez, M. Moliner, *Nature* **443** (2006) 842.
- [12] (a) B. Jandeleit, D.J. Schaefer, T.S. Powers, H.W. Turner, W.H. Weinberg, *Angew. Chem. Int. Ed.* **38** (1999) 2494;
(b) S.M. Senkan, *Angew. Chem. Int. Ed.* **40** (2001) 312;
(c) M.T. Reetz, *Angew. Chem. Int. Ed.* **40** (2001) 284;
(d) J.M. Newsam, F. Schuth, *Biotechnol. Bioeng.* **61** (1999) 203;
(e) F. Gennari, P. Seneci, S. Miertus, *Catal. Rev.-Sci. Eng.* **42** (2000) 385;
(f) W.F. Maier, K. Stöwe, S. Sieg, *Angew. Chem. Int. Ed.* **46** (2007) 6016;
(g) O.B. Vistad, D.E. Akporiaye, K. Mejlund, R. Wendelbo, A. Karlsson, M. Plassen, K.P. Lillerud, *Stud. Surf. Sci. Catal.* **154** (2004) 731;
(h) A. Cantín, A. Corma, M.J. Díaz-Cabañas, J.L. Jordá, M. Moliner, *J. Am. Chem. Soc.* **128** (2006) 4216;
(i) J.R. Hendershot, C.M. Snively, J. Lauterbach, *Chem. Eur. J.* **11** (2005) 806;
- (j) R.A. Potyrailo, W.F. Maier (Eds.), *Combinatorial and High-Throughput Discovery and Optimization of Catalysts and Materials*, Taylor & Francis, New York, 2006.
- [13] (a) E. Burello, G. Rothenberg, *Int. J. Mol. Sci.* **7** (2006) 375;
(b) J. Bajorath, *Nat. Rev. Drug Discov.* **1** (2002) 882;
(c) J.A. Hageman, J.A. Westerhuis, H.-W. Fruehauf, G. Rothenberg, *Adv. Synth. Catal.* **348** (2006) 361;
(d) E. Burello, G. Rothenberg, *Adv. Synth. Catal.* **347** (2005) 1969.
- [14] (a) C. Klanner, D. Farrusseng, L.A. Baumes, M. Lengliz, C. Mirodatos, F. Schüth, *Angew. Chem. Int. Ed.* **43** (2004) 5347;
(b) F. Schüth, L.A. Baumes, F. Clerc, D. Demuth, D. Farrusseng, J. Llamas-Galilea, C. Klanner, J. Klein, A. Martínez-Joaristi, J. Procelewska, M. Saupe, S. Schunk, M. Schwickardi, W. Strehlau, T. Zech, *Catal. Today* **117** (2006) 284.
- [15] C.T. Kresge, M.E. Leonowicz, W.J. Roth, J.C. Vartuli, J.S. Beck, *Nature* **359** (1992) 710.
- [16] T. Maschmeyer, F. Rey, G. Sankar, J.M. Thomas, *Nature* **378** (1995) 159.
- [17] (a) R. Millini, E. Previde-Massara, G. Perego, G. Bellussi, *J. Catal.* **137** (1992) 497;
(b) G. Bellussi, A. Carati, G.M. Clerici, G. Maddinelli, R. Millini, *J. Catal.* **133** (1992) 220.
- [18] (a) J.N. Cawse, M. Baerns, M. Holena, *J. Chem. Inf. Comput. Sci.* **44** (2004) 143;
(b) A. Tompos, J.L. Margitfalvi, E. Tfirst, L. Végvári, *Appl. Catal. A* **303** (2006) 72;
(c) L.A. Baumes, *J. Comb. Chem.* **8** (2006) 304;
(d) M. Holena, in: A. Hagemayer, P. Strasser, A.F. Volpe (Eds.), *High-Throughput Screening in Chemical Catalysis*, Wiley-VCH, Weinheim, 2004, p. 153;
(e) J.N. Cawse (Ed.), *Experimental Design for Combinatorial and High Throughput Materials Development*, John Wiley & Sons, New York, 2003.
- [19] (a) C. Bishop, *Neural Networks for Pattern Recognition*, University Press, Oxford, 1995;
(b) J. Zupan, J. Gasteiger, *Neural Networks in Chemistry and Drug Design: An Introduction*, Wiley-VCH, Weinheim, 1999.
- [20] (a) T.R. Cundari, J. Deng, Y. Zhao, *Ind. Eng. Chem. Res.* **40** (2001) 5475;
(b) L.A. Baumes, D. Farrusseng, M. Lengliz, C. Mirodatos, *QSAR Comb. Sci.* **29** (2004) 767;
(c) A. Corma, M. Moliner, J.M. Serra, P. Serna, M.J. Díaz-Cabañas, L.A. Baumes, *Chem. Mater.* **18** (2006) 3287;
(d) T. Hattoria, S. Kitob, *Catal. Today* **111** (2006) 328;
(e) S. Kito, T. Hattori, Y. Murakami, *Appl. Catal. A* **114** (1994) 173;
(f) L.A. Baumes, M. Moliner, A. Corma, *QSAR Comb. Sci.* **26** (2007) 255;
(g) Y. Watanabe, T. Umegaki, M. Hashimoto, K. Omata, M. Yamada, *Catal. Today* **89** (2004) 455;
(h) K. Omata, Y. Watanabe, M. Hashimoto, T. Umegaki, M. Yamada, *Ind. Eng. Chem. Res.* **43** (2004) 3282.
- [21] (a) L.A. Baumes, J.M. Serra, P. Serna, A. Corma, *J. Comb. Chem.* **8** (2006) 583;
(b) J.M. Serra, L.A. Baumes, M. Moliner, P. Serna, A. Corma, *Comb. Chem. High Throughput Screening* **10** (2007) 13.
- [22] J.M. Serra, A. Corma, A. Chica, E. Argente, V. Botti, *Catal. Today* **81** (2003) 393.
- [23] R. Todeschini, V. Consonni, in: R. Mannhold, H. Kubinyi, H. Timmerman (Eds.), *Handbook of Molecular Descriptors*, in: Series of Methods and Principles in Medicinal Chemistry, vol. 11, Wiley-VCH, Weinheim, 2000, p. 667.
- [24] (a) M.L. Drummond, B.G. Sumpter, *Inorg. Chem.* **46** (2007) 8613;
(b) I.V. Tetko, J. Gasteiger, R. Todeschini, A. Mauri, D. Livingstone, P. Ertl, V.A. Palyulin, E.V. Radchenko, N.S. Zefirov, A.S. Makarenko, V.Y. Tanchuk, V.V. Prokopenko, *J. Comput. Aided Mol. Des.* **19** (2005) 453;
(c) <http://www.vcclab.org/lab/edragon>.
- [25] A. Hunter, L. Kennedy, J. Henry, I. Ferguson, *Comput. Methods Programs Biomed.* **62** (2000) 11.
- [26] D.M. Hawkins, *J. Chem. Inf. Comput. Sci.* **44** (2004) 1.
- [27] A. Corma, V. Fornés, S.B. Pergher, Th.L.M. Maesen, J.G. Buglass, *Nature* **396** (1998) 353.
- [28] <http://www.topcombi.org>.